RSC Advances

ROYAL SOCIETY OF CHEMISTRY

www.rsc.org/advances

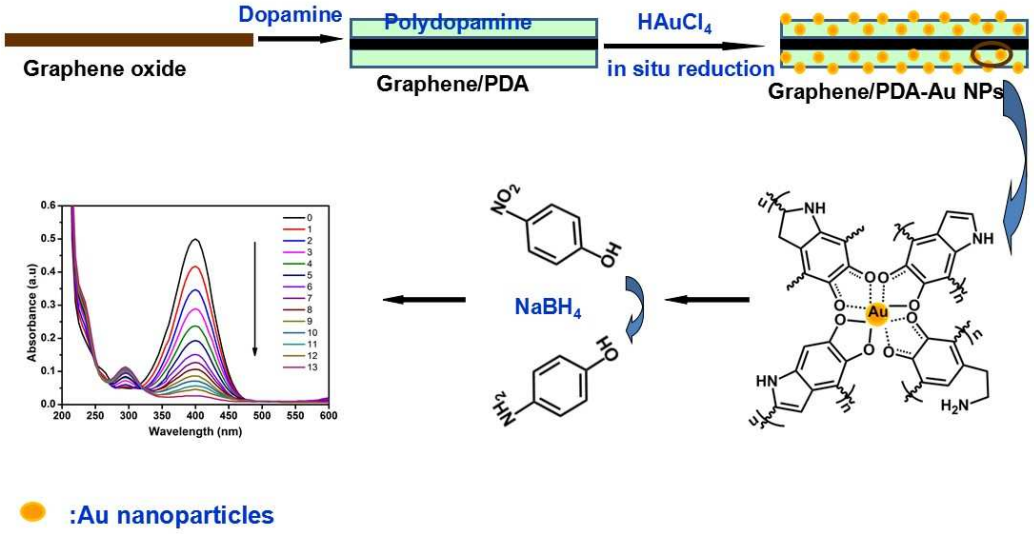

A simple, green and controllable route was demonstrated to prepare graphene/Au NPs nanocomposite using polydopamine as surface modifier, reducing agent and stabilizer simultaneously, avoiding the use of additional reducing agent and toxic reagents. The obtained graphene/PDA-Au NPs nanocomposite, combining the advantage of graphene and Au NPs, exhibits remarkable catalytic activity for the reduction of 4-nitrophenol to 4-aminophenol.

In situ green synthesis of Au nanoparticles onto polydopamine-functionalized graphene for catalytic reduction of nitrophenol

Jing Luo*, Nan Zhang, Ren Liu and Xiaoya Liu*

The Key Laboratory of Food Colloids and Biotechnology, Ministry of Education, School of Chemical and Material Engineering, Jiangnan University, Wuxi, Jiangsu, China 214122

Abstract: In this paper, a simple, green and environment-friendly method is developed for depositing gold nanoparticles (Au NPs) on the surface of polydopamine (PDA)-functionalized graphene (graphene/PDA) for highly efficient catalysis. In this approach, graphene/PDA was prepared through the self-polymerization of dopamine in the presence of graphene oxide (GO) in aqueous solution. With the addition of $HAuCl_4$, $AuCl_4^{-1}$ ions were adsorbed on the surface of graphene/PDA and in situ reduced to metallic Au NPs owing to the abundant catechol groups on PDA chain. In the whole procedure, PDA not only acts as the surface modifier of graphene, more importantly, it also serves as the reducing agent and stabilizer for Au NPs simultaneously, avoiding the usage of any toxic reducing reagent or special stabilizing agent. The graphene/PDA-Au NPs were characterized by Fourier transform infrared spectroscopy (FTIR), transmission electron microscopy (TEM), X-Ray Diffraction (XRD) and X-ray photoelectron spectroscopy (XPS). It was found that the size and amount of Au NPs are tunable by changing the experimental conditions. The obtained graphene/PDA-Au NPs nanocomposite, combining the advantage of graphene and Au NPs, exhibits remarkable catalytic activity for the reduction of 4-nitrophenol to 4-aminophenol. Considering its green facile preparation procedure and high catalytic activity, the prepared graphene/PDA-Au NPs holds great promise as a highly efficient,

*Corresponding author. Tel: Telephone: 86-510-85917763. Fax: 86-510-85917763. E-mail: jingluo19801007@126.com (J.Luo); lxy@jiangnan.edu.com (X. Liu).

cost-effective and environmental-friendly catalyst for industrial applications.

Keywords: Gold nanoparticles, graphene, polydopamine, catalyst

Introduction

During the past years, the synthesis of gold nanoparticles (Au NPs) has attracted considerable attention in both fundamental and application research due to their unique optical, catalytic, and electrochemical properties, compared to bulk metals, which endowed them with potential in a wide range of applications.[1-3] Especially, Au NPs have been proven as a high efficient catalyst.[4-5] Up to now, various methods have been developed for preparing Au NPs, among which the chemical reduction of $HAuCl_4$ in a solution using reducing reagent is the most common preparation procedure.[6-7] However, Au NPs in solution are unstable and susceptible to aggregation due to their high surface energy resulting from the high surface-to-volume ratio, which leads to remarkable reduction in catalytic activity.[8-9] So far, deposition of Au NPs onto various supporting matrix to generate hybrid catalysts has been recognized as an effective strategy to solve this problem. The solid supporting matrix that has been commonly used to protect against Au NPs aggregation includes polymer colloids [10], hydrogel [11-12], carbon materials [13], silica particles [14], metal oxides [15], and magnetic materials [16-17]. By tuning the surface functionality of the supporting materials, not only the maximal loading of the catalysts can be achieved, but also the strong synergistic interaction between Au NPs and the supporting materials can greatly enhance the catalytic activity and stability.

Graphene, a two-dimensional (2D) plate-like structure, is an attractive choice as the supporting matrix for anchoring nanoparticles, due to its large surface area (~2600 m^2/g), high chemical stability and unique mechanical properties.[18] The integration of graphene sheets with Au NPs may open up a new route for the preparation of the next generation catalysts. To date, a number of studies on the synthesis of nanocomposites integrating graphene and Au NPs have been reported with enhanced catalytic and electrochemical properties [19-22]. However, in most of these reports, the synthetic methods relied heavily on the use of toxic or hazardous chemical reducing agents,

such as sodium borohydride and hydrazine, during the chemical reduction process of both GO to graphene and $HAuCl_4$ to Au, which results in environmental and health risks. In addition, some tedious steps and drastic reaction conditions (long time, high temperature, organic solvents) were frequently required, which pose a significant hurdle for the large-scale preparation of graphene/Au NPs composites. Therefore, developing a simple and environmental friendly way to synthesize graphene/Au NPs composites with high performance becomes very desired.

Dopamine (DA) is a natural catecholamine neurotransmitter which contains both catechol and amine functional groups. In recent years, it was reported that DA could self-polymerize at weakly alkaline pH aqueous solution and spontaneously form a layer of multifunctional biocompatible polydopamine (PDA) film which adhere firmly to virtually any material of either inorganic and organic origins [23-26]. Besides its biocompatibility and adhesiveness, PDA has demonstrated good reducing ability due to the presence of a large number of catechol groups in PDA chain, which can be used to synthesize metal NPs from the reduction of metal salts. A variety of metal NPs including Au, Ag, Pt and Cu have been successfully synthesized and deposited on PDA functionalized surfaces without the need for extra reducing agent [17, 23, 27-29]. Besides reducing metal salts, it is recently found that polydopamine could function as a reducing agent for transforming graphene oxide (GO) to graphene and as a capping agent to stabilize and decorate the resulting reduced GO (RGO) in aqueous solution [30-33].

In this work, exploiting the advantages of PDA and graphene, we demonstrate a simple, convenient and green strategy to deposit Au NPs on PDA functionalized graphene with the use of PDA as a reducing and immobilizing agent simultaneously in aqueous media. In our approach, neither additional reducing agent nor the surface modifier is needed. In addition, the whole synthetic process was carried out in aqueous solution at ambient conditions without the need of heating, which is compatible with green chemistry principles. The main physical and chemical properties of the prepared graphene/PDA-Au NPs were fully characterized. At the same time, both the size and density of Au NPs are tunable by changing the

experimental conditions. The obtained graphene/PDA-Au NPs composites were employed as catalyst for the reduction of nitrobenzene. It was found that graphene/PDA-Au NPs showed high catalytic activity, which is strongly dependent on the particle size of Au NPs on graphene sheets. All these features make this simple and green procedure a potential route for the fabrication of low cost and high-performance catalyst.

Experimental

Reagents

Graphite powder, dopamine hydrochloride (DA), hydrogen tetrachloroaurate hydrate ($HAuCl_4 \cdot H_2O$), 4-nitrophenol (4-NP) and sodium hydroxide ($NaBH_4$) were purchased from Shanghai Alladin Chemical Reagents Company (Shanghai, China). All chemical reagents were used as received without further purification and were of analytical grade. The ultra-pure deionized water was used throughout the work.

Characterization

UV-vis spectrum was performed on a TU-1901 spectro-photometer (Beijing Purkinje General Instrument Co., Ltd.). FT-IR spectroscopic analyses were performed in reflection configuration with an FTLA 2000-104 FT-IR spectrometer in the 4000 to 400 cm^{-1} spectral domain with a spectral resolution of 4 cm^{-1}. The FT-IR analyses were performed on the mixture of the powder with KBr pressed into pellets. Measurements of Raman spectroscopy were carried out with a Renishaw in Via Raman Microscope operating at 514 nm with a charge-coupled device detector. TEM measurements were carried on a JEOL JEM-2100 microscope operating at 200 KV (JEOL, Japan). XRD profiles of Cu-modified graphene were obtained (XD-3A, Shimadzu) with high-intensity Cu Kα radiation (λ = 1.5406 nm). Crystallographic identification was accomplished by comparing the experimental XRD patterns with those of JCPDS database for standard inorganic crystal structures. XPS measurement was made on a VG ESCALAB MkII spectrometer with a Mg Ka X-ray source (1253.6 eV photos). The X-ray source was operated at 14 kV and 20 mA.

Preparation of graphene/PDA-Au NPs nanocatalyst

Graphene oxide was firstly synthesized from natural graphite according to previous report.[34] To prepare graphene/PDA composites, 20 mg of GO was dispersed in 10 mL Tris buffer (pH 8.5, 10 mM, 2 mg/mL) by ultrasonication and 40 mg dopamine was then added. The mixture was stirred for 12 h at room temperature. The resultant product was separated and washed with water to remove the unreacted monomer. To deposit Au NPs on graphene/PDA, 20 mg of graphene/PDA was suspended in 15 mL $HAuCl_4$ aqueous solution and the mixture was stirred for 12 h at room temperature. The resultant graphene/PDA-Au NPs nanocomposite was separated and rinsed with water for three times, and then dried under vacuum. The graphene/PDA-Au NPs were coded as graphene/PDA-Au1, graphene/PDA-Au2, graphene/PDA-Au3 and graphene/PDA-Au4 composite according to the initial $HAuCl_4$ concentrations of 0.1, 0.25, 0.5 and 0.75 mg/mL.

Reduction of 4-nitrophenol by graphene/PDA-Au NPs

For the catalytic reduction of 4-nitrophenol, 1 mL of 4-nitrophenol aqueous solution (1 mM) was mixed with 25 mL of distilled water containing a certain amount of graphene/PDA-Au NPs nanocomposite. N_2 was then purged into the above suspension for half an hour to remove the dissolved O_2. Subsequently, 4 mL of fresh $NaBH_4$ aqueous solution (0.33 M) was injected to initiate the reduction reaction. The solution mixture was kept stirring during the reaction. According to Lambert-beer law, the absorbance of 4-nitrophenol is proportional to its concentration in the solution, so the ratio of absorbance intensity at time t (At) to that at t = 0 (A_0) should be equal to the concentration ratio C_t/C_0 of 4-nitrophenol. As a result, the progress of the reaction could be directly reflected by the change of the absorption intensity. Therefore, UV-vis spectrometry was employed to monitor the conversion progress of 4-nitrophenol to 4-aminophenol at a certain time interval at room temperature through measuring the decrease of absorbance at 400 nm. The catalyst was recovered by centrifugation and then washed with water.

Results and discussion

Synthesis and characterization of graphene/PDA-Au NPs

The schematic illustration of the preparation of graphene/PDA-Au NPs composites is demonstrated in Scheme 1. By mixing GO with a weak alkaline solution of DA, GO nanosheet was readily reduced to graphene accompanied by simultaneous formation of a thin polydopamine (PDA) film (from self-polymerization of dopamine) around the resulted graphene sheets surface. The obtained PDA functionalized graphene (graphene/PDA) was then immersed in $HAuCl_4$ solution, wherein $AuCl_4^-$ ions diffused into the PDA layer and subsequently reduced to Au^0 atoms by the catechol groups on PDA chains. Then the neighboring Au^0 atoms aggregate together to form Au nanoparticles which are stabilized by the catechol groups of PDA layer on surface of graphene, leading to the formation of graphene/PDA-Au NPs composites. The whole process did not require toxic reagents such as hydride or sodium borohydrate normally involved in the reduction of GO to graphene or $HAuCl_4$ to Au^0, with PDA serving as reductant not only for GO but also for $HAuCl_4$. In addition, neither additional surface modifier for graphene nor special stabilizer for Au NPs is needed. Furthermore, the reactions were environmental-friendly processes, which were conducted in aqueous media at ambient conditions, eliminating the use of organic solvent and thermal treatment.

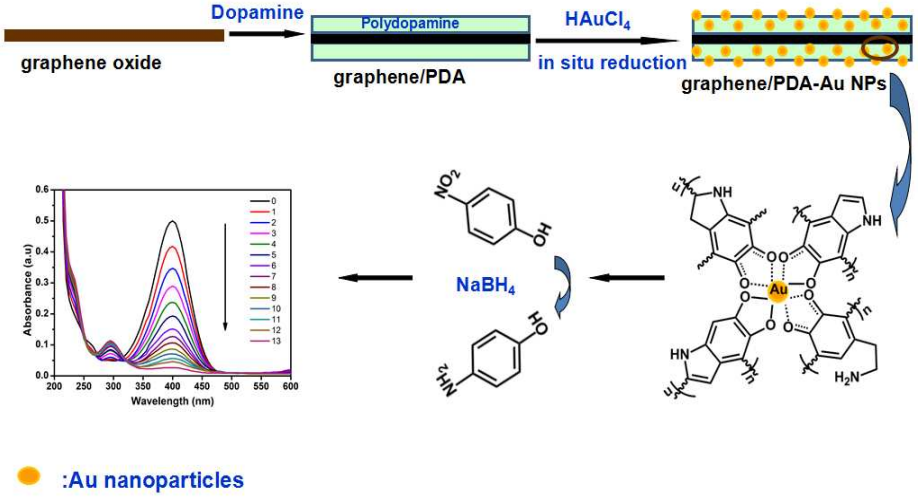

Scheme 1. Schematic illustration of the fabrication of graphene/PDA-Au NPs nanocomposite and application for catalyzing the reduction of 4-nitrophenol to 4-aminophenol

UV-vis measurement was firstly performed to characterize the formation of graphene/PDA-Au NPs nanocomposite. The UV-vis spectra of GO, graphene/PDA and graphene/PDA-Au NPs nanocomposite are shown in Fig. 1A. The spectrum of GO shows a maximum at 230 nm and a shoulder at 300 nm (curve a), which is ascribed to π-π* transitions of aromatic C=C bonds. The reduction of GO to graphene by PDA was evidenced by the blue-shift of the absorption band from 230 nm to 275 nm (curve b), indicating the restoration of the electronic conjugation within the graphene sheets.[35-36] The sharp peak at 208 nm is ascribed to the absorption of polydopamine.[37] After mixing graphene/PDA with $HAuCl_4$ solution, it is observed that a new broad absorbance band appears at about 560 nm (curve c) which is characteristic of colloidal gold surface plasmon resonance band [38-39], suggesting the formation of Au nanoparticles on the surface of graphene/PDA. Fig. 1B shows the FTIR spectra of GO, graphene/PDA and graphene/PDA-Au NPs. For the spectrum of graphene/PDA, the appearance of strong peaks at 1627 cm^{-1} and 1543 cm^{-1} are two typical absorption peaks of phenyl group, and the weak peaks at 1294 cm^{-1} and 1393 cm^{-1} are attributed to CH_2 scissoring vibration of PDA chain.[26,27] Two moderately intensive peaks are assigned to the in-plane bending vibrations of O–H and stretching vibration of C–OH at 1300 cm^{-1} and 1106 cm^{-1}, respectively. The band between 2800 cm^{-1} and 3400 cm^{-1} should be assigned to the stretching vibration of –OH (phenolic hydroxyl) or $–NH_2$. The above results provide evidence of the formation of PDA layer on the surface of graphene. In addition, the C=O peak at 1727 cm^{-1} in GO (curve a) disappeared in graphene/PDA, which indicated the reduction of GO [26].

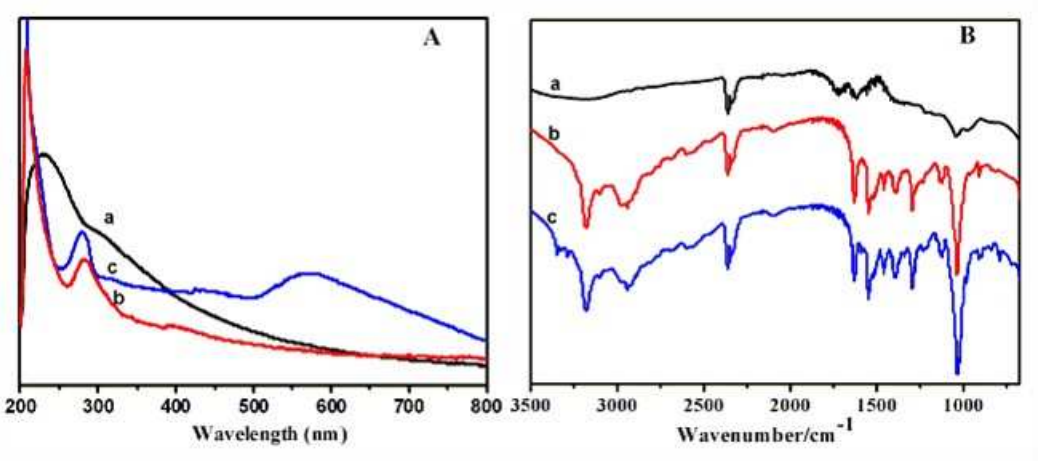

Fig. 1 UV-vis (A) and FTIR spectra (B) of (a) GO, (b) graphene/PDA and (c) graphene/PDA-Au NPs

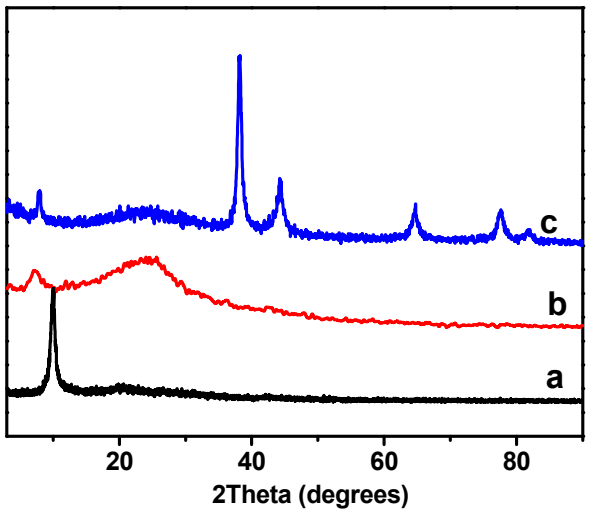

Fig. 2 XRD of (a) GO, (b) graphene/PDA and (c) graphene/PDA-Au NPs

Fig. 2 shows the XRD patterns of GO, graphene/PDA and graphene/PDA-Au NPs nanocomposite. It can be seen that the intense diffraction peak at 2θ = 9.2° characteristic of GO (curve a) decreased significantly and a new broad diffraction peak at 2θ = 24.5° has appeared in graphene/PDA (curve b). This diffraction peak was quite close to the typical diffraction peak of graphite at 2θ = 26.6°[40], implying the successful reduction of GO to graphene. In the patterns of graphene/PDA-Au NPs nanocomposite (curve c), four new peaks at 2θ of 38°, 43°, 65° and 78° appear, which

should be correspondingly assigned to the (1 1 1), (2 0 0), (2 2 0) and (3 1 1) crystal faces of Au nanoparticles (face centered cubic, JCPDS card no. 04-783) [41]. In addition, the characteristic broad peak of graphene at 24.5° was still present. These results confirm the successful preparation of graphene/PDA-Au NPs.

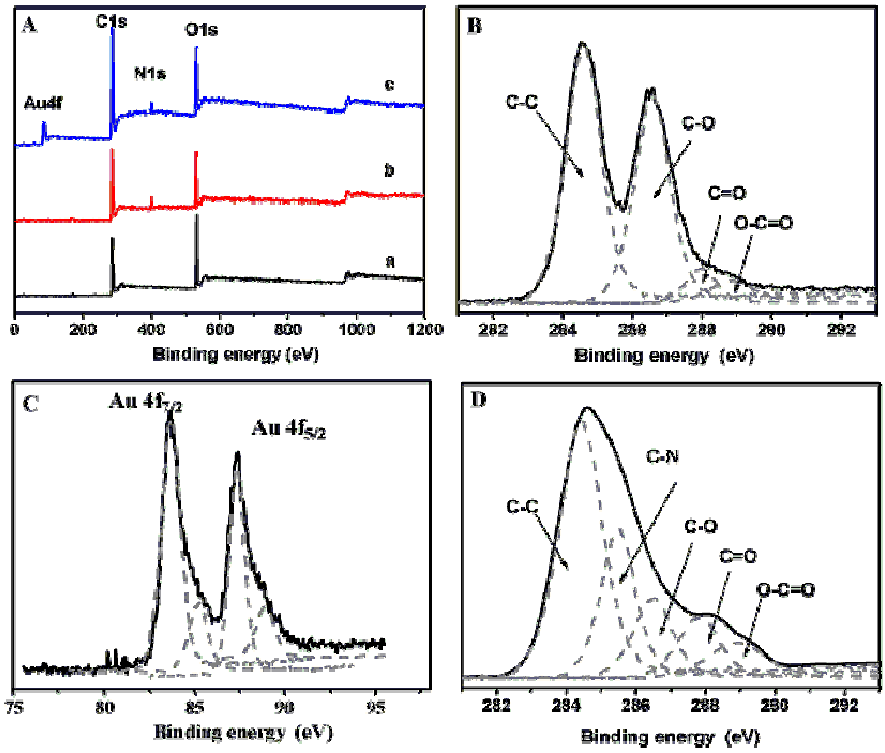

Fig. 3 (A) XPS survey spectra of (a) GO, (b) graphene/PDA and (c) graphene/PDA-Au NPs. (C) Au 4f core-level spectrum. XPS C 1s core-level spectra of GO (B) and graphene/PDA (D).

To further confirm the presence of PDA layer and the in situ formation of Au NPs on the surface of graphene, X-ray photoelectron spectroscopy (XPS) as a sensitive surface analytical tool was used to provide elemental information of the surface composition of graphene/PDA and graphene/PDA-Au NPs. Fig. 3 showed the XPS spectra of GO, graphene/PDA and graphene/PDA-Au NPs nanocomposite. GO exhibits the C 2p peak at 285 eV and O 2p peak at 527 eV (Fig. 3A, curve a) due to the existence of hydroxyl groups and carboxylic groups on its surface. The XPS C 1s core-level spectrum of GO (Fig. 3B) can be curved-fitted into four peak components

with binding energies at about 284.6, 286.4, 287.9, and 288.8 eV, corresponding to the C-C, C-O, C=O, and O-C=O species, respectively. The survey spectrum of the graphene/PDA (Fig. 3A, curve b) clearly showed a new peak at 401 eV which is attributed to N 1s, demonstrating successful formation of PDA layer on the surface of graphene. For graphene/PDA (Fig. 3D), its XPS C 1s core-level spectrum can be curved into five peak components with binding energies at about 284.6, 285.5, 286.4, 287.8, and 288.9 eV, assigned to the C-C, C-N, C-O, C=O, and O-C=O species, respectively [30]. Compared to GO, a significant decrease of C–O peak component at 286.4 eV, was observed for PDA@RGO, indicating the reduction of GO by dopamine. In addition, the appearance of the C-N peak component at the BE of 285.5 eV in the C 1s core-level spectrum is consistent with the presence of PDA layer. The XPS spectrum of graphene/PDA-Au NPs nanocomposite (Fig. 3A, curve c) clearly shows the signals for C, O, N, and Au element, confirming the successful formation of Au NPs on graphene/PDA. Fig. 3C displays the high-resolution spectrum for Au 4f. The binding energies at 83.7 and 87.3 eV are ascribed to Au $4f_{7/2}$ and Au $4f_{5/2}$ of the metallic Au, respectively. It should be noted that a small fraction of $Au^{+/3+}$ exists from the binding energies of Au^{+} $4f_{7/2}$ (85.3 eV) and Au^{3+} $4f_{7/2}$ (88.5 eV) [42, 43] in the XPS spectrum of Au, which is possibly attributed to physical absorption and incomplete reduction of $HAuCl_4$ by PDA.

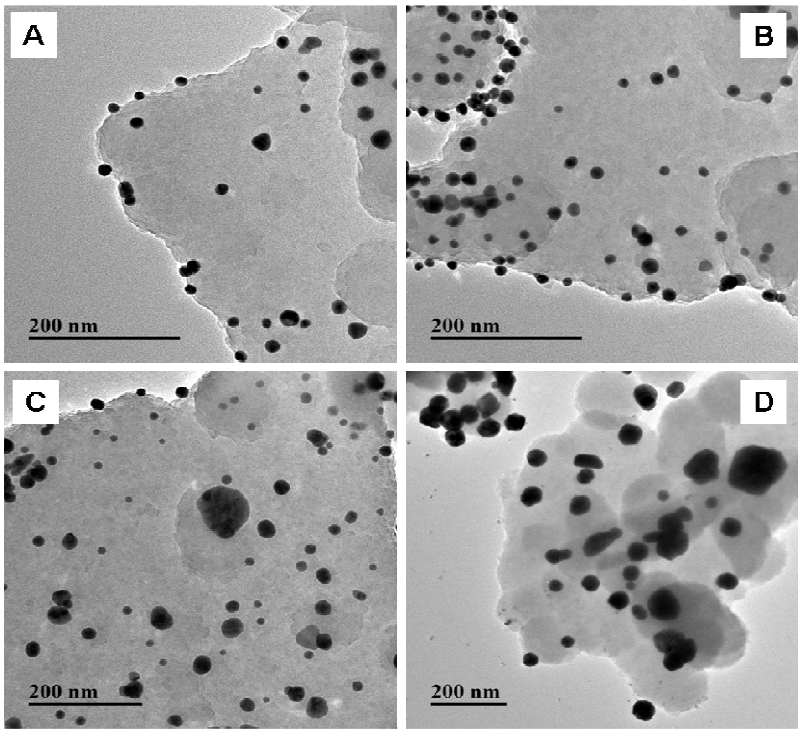

Fig. 4 TEM images of graphene/PDA-Au NPs nanocomposites with a different concentration of $HAuCl_4$: (A) 0.1 mg/ml (graphene/PDA-Au1), (B) 0.25 mg/ml (graphene/PDA-Au2), (C) 0.5 mg/ml (graphene/PDA-Au3), (D) 0.75 mg/ml (graphene/PDA-Au4).

The impact of $HAuCl_4$ concentration on the formation of graphene/PDA-Au NPs composite was revealed by the TEM images. Fig. 4 shows the representative TEM images of graphene/PDA-Au1, graphene/PDA-Au2, graphene/PDA-Au3 and graphene/PDA-Au4 composite from the initial $HAuCl_4$ concentrations of 0.1, 0.25, 0.5 and 0.75 mg/mL. It can be clearly observed that the size and amount of the Au NPs are strongly dependent on the concentration of $HAuCl_4$. When the concentration of $HAuCl_4$ is low (0.1 mg/mL), it is seen that a small amount of Au NPs are immobilized on the surface of graphene/PDA (Fig. 4A). With the concentration of $HAuCl_4$ increasing to 0.25 mg/mL, the amount of Au NPs on graphene/PDA increased obviously (Fig. 4B). These particles are generally spherical in shape with narrow size distribution. From the inserted particle size distribution diagram of the Au nanoparticles (Fig. 5B), it can be observed that the most distributed dimension is in the range of 10 – 20 nm and the mean particle diameter was about 16 nm. With the

further increasing concentration of $HAuCl_4$ (0.5 mg/ml), Au NPs with wider size distribution can be observed and some large metal aggregates also appear (Fig. 4C and Fig. 5C). When the concentration of $HAuCl_4$ is increased to 0.75 mg/ml, more large size Au NPs with different shapes are observed (Fig. 4D). The possible reason is that at high dosage of $HAuCl_4$, the redox reaction between catecholamine and $AuCl_4^-$ ions becomes faster which result in the uncontrolled deposition of Au particle. Evaluated from inductively coupled plasma-mass spectrometer (ICP-MS), the amount of Au immobilized on graphene/PDA was found to be about 1.4, 3.2, 4.5, and 5.6 wt % for the graphene/PDA-Au1, graphene/PDA-Au2, graphene/PDA-Au3 and graphene/PDA-Au4, respectively.

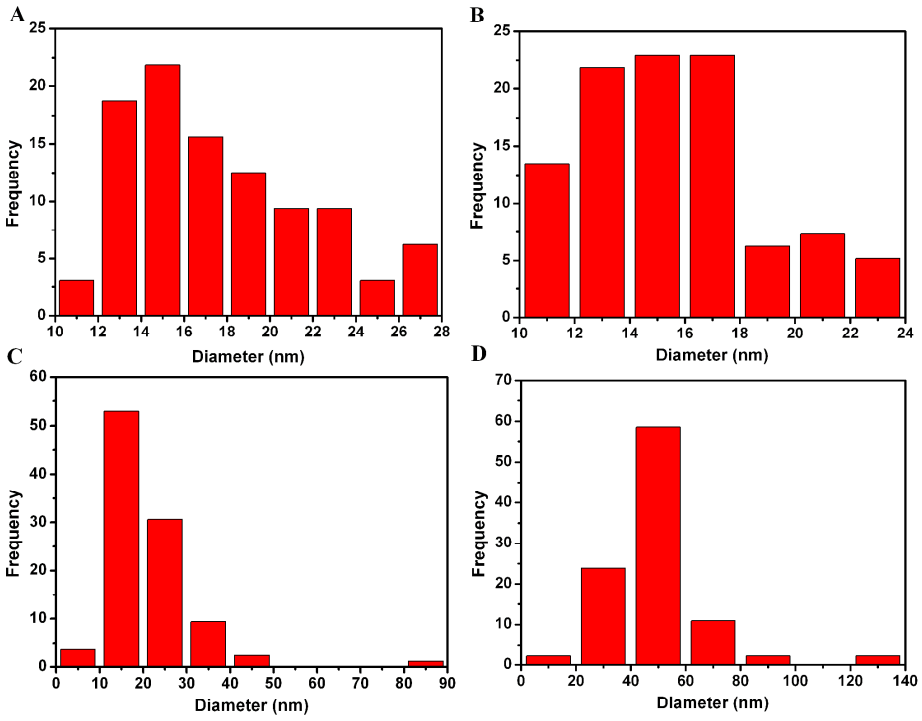

Fig. 5 The size distribution of the Au NPs for graphene/PDA-Au1 (A), graphene/PDA-Au2 (B), graphene/PDA-Au3 (C) and graphene/PDA-Au4 (D)

To evaluate the catalytic performance of graphene/PDA-Au NPs nanocomposites, the reduction of 4-nitrophenol to 4-aminophenol in the presence of $NaBH_4$ was chosen as a model system. The original 4-nitrophenol aqueous solution shows a typical absorption peak at 317 nm and its color is light yellow. With the addition of

$NaBH_4$, 4-nitrophenol aqueous solution turned to yellowish green and the absorption peak red-shifts to 400 nm, corresponding to the formation of 4-nitrophenolate in alkaline conditions.[44] After the addition of a small amount of graphene/PDA-Au NPs nanocomposites into the reaction system, the reduction process occurs and was monitored by measuring the UV-vis adsorption spectra of the reaction mixture with respect to time. Fig. 6 shows the changes in UV−visible absorption spectrum of the 4-nitrophenol and $NaBH_4$ reaction mixtures in the presence of graphene/PDA-Au NPs composite. It can be seen that the absorption intensity at 400 nm, ascribed to nitro compounds, decreases quickly with time and a new peak at 290 nm appeared due to the formation of 4-AP. Correspondingly, the yellow-green color of the reaction mixture faded with the progress of time. The above results demonstrate the succesful transformation of 4-nitrophenol to 4-aminophenol under the catalysis of graphene/PDA-Au NPs nanocomposite. In contrast, the absorption intensity at 400 nm was almost unchanged without the presence of graphene/PDA-Au NPs, indicating that it is difficult for the reduction to proceed without a catalyst. Control experiments were also carried out using bare graphene/PDA as catalyst instead of graphene/PDA-Au NPs. There was no color change of 4-aminophenol solution and no significant change in color or the absorption intensity at 400 nm even after 48 h, indicating the graphene/PDA has negligible catalytic effect on the reduction of 4-nitrophenol.

It is well-known that the catalytic property of Au nanoparticles is strongly dependent on their size and dispersity [45]. The above TEM images clearly exhibit that the size and dispersity as well as the shape of Au on graphene/PDA varied with the different concentration of $HAuCl_4$, which would endow different catalytic activity for the obtained graphene/PDA-Au NPs nanocomposite. Hence, the impact of $HAuCl_4$ concentration on the catalytic performance of graphene/PDA-Au NPs was also investigated. Fig. 6A-D provides the time-dependent UV-vis adsorption spectra of the reaction mixture catalyzed by graphene/PDA-Au1, graphene/PDA-Au2, graphene/PDA-Au3 and graphene/PDA-Au4. A reaction time of 18 min was required to achieve the full reduction of 4-nitrophenol using graphene/PDA-Au1 as catalyst (Fig. 6A). For graphene/PDA-Au2, a shorter time of 13 min was needed (Fig. 6B).

However, this time increased to 16 and 18 min for graphene/PDA-Au3 (Fig. 6C) and graphene/PDA-Au4 (Fig. 6D), respectively. The effect of graphene support on the catalytic activity was also investigated. Au nanoparticles alone were prepared by mixing $HAuCl_4$ with dopamine in weak alkaline aqueous solution. It take Au nanoparticles more than 30 min to achieve the full reduction of 4-nitrophenol (Fig. 6E), much longer than graphene/PDA-Au NPs, suggesting much lower catalytic activity of Au nanoparticles than graphene/PDA-Au nanocomposite for the reduction of 4-nitrophenol. This result showed that graphene support should play an important role in the catalysis, yielding a synergistic effect.

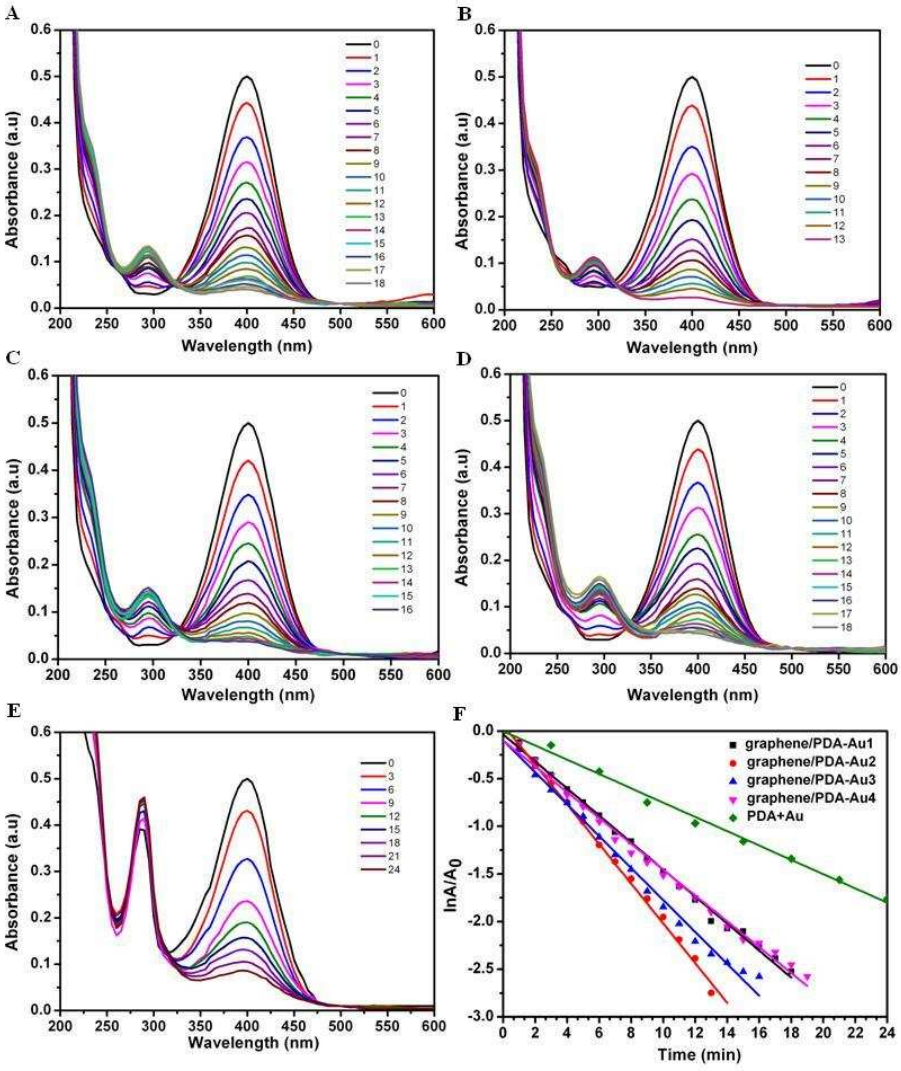

Fig. 6 UV-vis adsorption spectra of the reduction of 4-NP by $NaBH_4$ in the presence

of graphene/PDA-Au1 (A), graphene/PDA-Au2 (B), graphene/PDA-Au3 (C), graphene/PDA-Au4 (D) and PDA-Au (E); (F) plot of $\ln(C_t/C_0)$ of 4-NP against time for the catalysts.

Since the concentration of $NaBH_4$ is much higher than that of 4-nitrophenol, the rate of reduction of 4-nitrophenol is independent of the $NaBH_4$ concentration which allow this reaction to be evaluated by pseudo-first-order kinetics. The ratio of C_t (the initial concentration of 4-nitrophenol at reaction time t) to C_0 (the initial concentration of 4-nitrophenol) was calculated from the relative intensity ratio of the corresponding absorbance (A_t/A_0). Fig. 6F shows the $\ln(C_t/C_{0)}$ versus time for all catalyst systems (graphene/PDA-Au1-4 nanocomposites) and good linear relationships are observed, indicating that the reduction of 4-nitrophenol to 4-aminophenol follows the pseudo-first-order kinetics. The kinetic reaction rate constants (k) were determined from the slope of the straight line which is 0.14 min^{-1} for graphene/PDA-Au1, 0.225 min^{-1} for graphene/PDA-Au2, 0.18 min^{-1} for graphene/PDA-Au3, and 0.14 min^{-1} for graphene/PDA-Au4, respectively. This result means that graphene/PDA-Au2 possess the faster reduction rate and thus higher catalytic activity for the reduction of 4-nitrophenol, which should be attributed to the size and density effect of Au NPs in the graphene/PDA-Au NPs nanocatalyst. It can be observed from TEM images that compared with graphene/PDA-Au1, graphene/PDA-Au3 and graphene/PDA-Au4, more and smaller Au NPs were deposited on graphene surface in graphene/PDA-Au2, which would significantly enhance the accessibility of 4-nitrophenol to catalytic sites and thus enhance the catalytic performance. Therefore, the concentration of $HAuCl_4$ contributed a lot in controlling the formation of Au NPs and greatly affects the catalytic activity. In order to compare our results with reports in the literature, the ratio of rate constant k over the total weight of the graphene/PDA-Au catalyst, $k_0 = k/m$, was calculated. The catalytic activity factor k_0 of the graphene/PDA-Au2 was 0.225 min^{-1} / 1.25 mg = 3.0 s^{-1}/g, which is higher than that of previously reported spongy Au nanoparticles (0.35 s^{-1}/g) [46]. In addition, it is also larger than the highest value reported among the polymer reported Au nanoparticles catalysts (2.26 s^{-1}/g) [47].

In addition, considering different conditions and different Au amount for different catalyst systems, we use the turnover frequency (TOF) to determine the efficiency of our graphene/PDA-Au catalyst for 4-nitrophenol reduction and compare with previously reported Au based nanocatalysts[8, 16, 47-53] based on gold amount. The turnover frequency (TOF) of graphene/PDA-Au catalyst is 0.38 min^{-1}, calculated by the moles of 4-NP reduced per mole of Au per consumed time under the present reaction conditions. As shown in Table S1, in comparison with other Au based catalysts, our graphene/PDA-Au catalyst showed a higher catalytic efficiency than most of other Au based catalysts for the reduction of 4-nitrophenol. Although much higher TOFs of Yolk-double shell SiO_2@Fe_3O_4-C@Au [16] and Fe_3O_4@SiO_2-LBL-Au [52] have been reported (Table S1), our graphene/PDA-Au catalyst has the advantages of simple synthetic procedure and mild preparation conditions.

The above results showed that graphene/PDA-Au NPs possessed superior high catalytic activity, which should be attributed to the synergistic effect of graphene sheet and Au NPs, explained as following: (1) As 4-NP is p-rich in nature, it is expected graphene can highly adsorb 4-NP via $\pi - \pi$ stacking interactions, leading to a high concentration of 4-NP near to the Au nanoparticles on graphene sheet and thus an efficient contact between 4-NP and Au nanoparticles. Whereas for the pure Au nanoparticles without graphene as the support, 4-NP may collide with Au nanoparticles by chance, leading to inefficient contact between 4-NP and Au nanoparticles. (2) The narrow size distribution, uniform distribution and good crystal structure of Au NPs for the graphene/PDA-Au2 are beneficial to catalyzing the reaction efficiently. (3) As reported in many literatures, there exist the electron transfer from graphene and Au NPs, which can increase the local electron concentration and facilitate the uptake of electrons by 4-NP molecules in several publications [53-54].

To investigate the reusability of our catalyst, successive cycles of the catalytic reduction were carried out using graphene/PDA-Au2 as example. Our graphene/PDA-Au2 nanocatalyst could be recovered by brief centrifugation or filtered and reused for three successive cycles of reaction with a conversion efficiency of

around 100%, indicating the stable and high recycling efficiency of the graphene/PDA-Au2. It should be noted that the reaction time increased from 13 min to 25 min and the rate constant rapidly decreased from 0.225 min^{-1} to 0.12 min^{-1} when the graphene/PDA-Au2 catalyst was reused for the first cycle. But interestingly, the k values for the subsequent three cycles kept almost unchanged. To exclude the possible reasons such as gold sintering and gold leaching, the graphene/PDA-Au2 recycled after each run was analyzed by ICP-AES and no great Au loss on used catalyst was found, indicating no detachment of Au NPs during the catalytic reaction. In addition, TEM images (Fig. S1) showed that the size of Au NPs kept almost unchanged, indicating no aggregation or sintering of Au NPs occured in the graphene/PDA-Au2. Similar recycling catalytic behaviors have been recently reported using Ag@alginate hydrogel [11] and poly(N-isopropylacrylamide)/Au nanocomposites [55] as catalyst. The decreased rate constant for the reduction reaction is possibly caused by the absorption of the catalytic reduction product (4-aminophenol) onto the Au NPs at the graphene/PDA-Au NPs interface. It is known that the amine groups in 4-aminophenol have a strong affinity to the surface of Au NPs,[16,50] which can prevent the reactant (4-nitrophenol) from reaching Au NPs. As a result, the catalytic activity of graphene/PDA-Au NPs decreased for the first cycle. The almost unchanged rate constant for the subsequent cycles is possibly attributed to the similar concentration gradient of 4-aminophenol around graphene/PDA-Au NPs for each cycle and thus the same diffusion behavior of the reactant (4-nitrophenol) to Au NPs in graphene/PDA-Au NPs.

.

Conclusions

In summary, a simple, green and controllable route was demonstrated to prepare graphene/Au NPs nanocomposite using polydopamine as surface modifier, reducing agent and stabilizer simultaneously, avoiding the use of additional reducing agent and toxic reagents. The obtained graphene/PDA-Au NPs nanocomposite was fully characterized and exhibits good catalytic activity for the reduction of 4-nitrophenol to

4-aminophenol. In addition, the coverage, size and morphology of the Au NPs on the surface of graphene can be facilely tailored through the adjustment of the concentration of $HAuCl_4$, which has a direct influence on the catalytic activity of the graphene/PDA-Au NPs.

Acknowledgement

We acknowledge financial support from the National Natural Science Foundation of China (under Grant Nos. 51103064 and 21174056), the Fundamental Research Funds for the Central Universities (JUSRP 51305A), MOE & SAFEA for the 111 Project (B13025).

.

References

1. P. K. Jain, X. Huang, I. H. Ei-sayed, M. A. EI-Sayed, *ACR*, 2008, 41, 1578-1586.

2. B. Lim, M. Jiang, P. H. C. Camargo, E. C. Cho, J. Tao, X. Lu, Y. Zhu, Y. Xia, *Science*, 2009, 324, 1302-1305.

3. C. M. Cobley, J. Chen, E. C. Cho, L. Wang, Y. Xia, *Chem. Soc. Rev.*, 2011, 40, 44-56.

4. J. John, E. Gravel, A. Hagege, H. Y. Li, T. Gacoin, E. Doris, *Angew. Chem.*, 2011, 123, 7675-7678.

5. M. Grzelczak, J. Perez-Juste, P. Mulvaney, L. M. Liz-Marzan, *Chem. Soc. Rev.*, 2008, 37, 1783-1791.

6. M. C. Daniel, D. Astruc, *Chem. Rev.*, 2004, 104, 293-346

7. M. Na, L. Jun, Z. Wang, *Chin. J. Anal. Chem.*, 2010, 38, 1~7.

8. H. Wu, X. Huang, M. Gao, X. Liao, B. Shi, *Green Chem.*, 2011, 13(3), 651-658.

9. Z. Jin, M. Xiao, Z. Bao, P. Wang, J. Wang, A*ngew. Chem. Int. Ed.*, 2012, 51, 6406-6410.

10. S. Wu, J. Dzubiella, J. Kaiser, M. Drechsler, X. Guo, M. Ballauff, Y. Lu, *Angew. Chem. Int.*, *Ed.* 2012, 51, 2229-2233

11. L. Ai, H. Yue, J. Jiang, *J. Mater. Chem.*, 2012, 22, 23447-23453.

12. B. Adhikari, A. Biswas, A. Banerjee, *ACS Appl. Mater. Interfaces*, 2012, 4,

5472-5482.

13 K. K. R. Datta, B. V. Subba Reddy, K. Ariga, Ajayan Vinu, *Angew. Chem. Int. Ed.*, 2012, 51, 2229-2233.

14. L. You, Y. Mao, J. Ge, *J. Phys. Chem. C*, 2012, 116, 10753-10759.

15. Z. Seh, S. Liu, S. Zhang, K. W. Shah, M. Han, *Chem. Commun.*, 2011, 47, 6689-6691.

16 T. Zeng, X. Zhang, S. Wang, Y. Ma, H. Niu, Y. Cai, *J. Mater. Chem. A*, 2013, 1, 11641–11647

17. T. Zeng, X. Zhang, H. Niu, Y. Ma, W. Li, Y. Cai, *Appl. Catal. B: Environ.*, 2013, 134, 26-33.

18. A. K. Geim, *Science*, 2009, 324, 1530-1534.

19. C. Zhu, L. Han, P. Hu, S. Dong, *Nanoscale*, 2012, 4, 1641-1646.

20. T. Wu, L. Zhang, J. Gao, Y. Liu, C. Gao, J. Yan, J. *Chem. Mater. A*, 2013, 1, 7384-7390.

21. S. Li, S. Guo, H. Yang, G. Gou, R. Ren, J. Li, Z. Dong, J. Jin, J. Ma, *J Hazard. Mater.*, 2014, 270, 11-17.

22. X. Qin, W. Lu, A. M. Asiri, A. O. Al-Youbi, X. Sun, *Catal. Sci. Technol.*, 2013, 3, 1027-1035

23. H. Lee, S. M. Dellatore, W. M. Miller, P. B. Messersmith, *Science*, 2007, 318, 426-430.

24. H. Lee, B. Lee, P. B. Messersmith, *Nature*, 2007, 448, 338-341.

25. H. Lee, Y. Lee, A. R. Statz, J. Rho, T. G. Park, P. B. Messersmith, *Adv. Mater.*, 2008, 20, 1619-1623.

26. S. Kang, N. Hwang, J. Yeom, S. Y. Park, P. B. Messersmith, I. S. Choi, R. Langer, D. G. Anderson, H. Lee, *Adv. Funct. Mater.*, 2012, 22, 2949-2955.

27. B. Fei, B. Qian, Z. Yang, R. Wang, W. Liu, C. Mak, J. Xin, *Carbon*, 2008, 46, 1795-1797.

28. K. C. L. Black, Z. Liu, P. B. Messersmith, *Chem. Mater.*, 2011, 23, 1130-1135.

29. M. Sureshkumar, D. Y. Siswanto, C. Lee, *J. Mater. Chem.*, 2010, 20, 6948-6955.

30. L. Xu, W. Yang, K. G. Neoh, E. Kang, G. Fu, *Macromolecules*, 2010, 43,

8336-8339.

31. S. Kang, S. Park, D. Kim, S. Y. Park, R. S. Ruoff, H. Lee, *Adv. Funct. Mater.*, 2011, 21, 108-112.

32. L. Yang, W. A. Yee, S. L. Phua, J. Kong, H. Ding, J. W. Cheah, X. Lu, *RSC Adv.*, 2012, 2, 2208-2210.

33. L. Guo, Q. Liu, G. Li, J. Shi, J. Liu, T. Wang, G. Jiang, *Nanoscale*, 2012, 4, 5864-5867.

34. J. Luo, S. Jiang, H. Zhang, J. Jiang, X. Liu, *Anal. Chim. acta*, 2012, 709, 47-53.

35. D. Li, M. B. Muller, S. Gilje, R. B. Kaner, G. G. Wallace, *Nat. Nanotechnol.*, 2008, 3, 101-105.

36. B. S. Kong, J. X. Geng, H. T. Jung, *Chem. Commun.*, 2009 , 2174-2176.

37. J. Luo, S. Jiang, X. Liu, *J. Phys. Chem. C*, 2013, 117, 18448-18456.

38. S. Tan, M. J. Campolongo, D. Luo, W. Cheng, *Nat. Nanotechnol.*, 2011, 6, 268-276.

39. M. Iliut, C. Leordean, V. Canpean, C. M. Teodorescu, S. Astilean, *J. Mater. Chem. C*, 2013, 1, 4094-4104.

40. J. Zhang, H. Yang, G. Shen, P. Cheng, J. Zhang, S. Guo, *Chem. Commun.*, 2010, 46, 1112-1114.

41. Joint Committee on Powder Diffraction Standards (JCPDS) 04–784.

42. M. P. Casaletto, A. Longo, Martorana, Prestianni, A. M. Venezia, 2006, 38, 215–218.

43. Z. Zheng, B. Huang, X. Qin, X. Zhang, Y. Dai, M. H. Whangbo, *J. Mater. Chem.*, 2011, 21, 9079.

44. B. Adhikari, A. Biswas, A. Banerjee, *ACS Appl. Mater. Interfaces*, 2012, 4, 5472-5482.

45. L. Chen, J. Hu, R. Richards, *J. Am. Chem. Soc.*, 2008, 131, 914-915.

46. H. MdRashid, R. R. Bhattacharjee, *Langmuir*, 2006, 22, 7141-7143.

47. K. Kuroda, T. Ishida, M. Haruta, *J. Mol. Catal. A: Chem.*, 2009, 298, 7-11.

48. S. Wu, C. Tseng, Y. Lin, C. Lin, Y. Hung, C. Mou, *J. Mater. Chem.*, 2011, 21, 789-794.

49. T. Zeng, X. Zhang, H. Niu, Y. Ma, W. Li, Y. Cai, *Appl. Catal. B: Environ.*, 2013, 134-135.

50. F. Lin, R. Doong, *J. Phys. Chem. C*, 2011, 115, 6591-6598.

51. Y. Deng, Y. Cai, Z. Sun, J. Liu, C. Liu, J. Wei, W. Li, C. Liu, Y. Wang, D. Zhao, *J. Am. Chem. Soc.*, 2010, 132, 8466-8473.

52. Y. Zhu, J. Shen, K. Zhou, C. Chen, X. Yang, C. Li, *J. Phys. Chem. C*, 2011, 115, 1614-1619.

53. J. Li, C. Liu, Y. Liu, *J. Mater. Chem.*, 2012, 22, 8426-8430.

54. S. Li, S. Guo, H. Yang, G. Gou, R. Ren, J. Li, Z. Dong, J. Jin, J. Ma, J. *Hazard. Mater.*, 2014, 270, 11-17.

55. C. Zhu, Z. Hai, H. Li, J. Chen, S. Yu, *Small*, 2012, 8, 930-936.